Journal of Applied Geophysics (Cairo) Vol. 22, Issu.1, May (2023) (p.p., 1-16)

ISSN: 1687-1251

Egyptian Society of Applied Petrophysics

Journal of Applied Geophysics (Cairo)

Journal home page: https://jag.journals.ekb.eg/

Original Article

Assessment of the Geo-Engineering Suitability of Subsurface Layers Using ERT and SSR, A case study: Combined Services Area of "Madinaty", New Cairo, Egypt

Alhussein Adham Basheer [1*], Raghda M. Abd Elhamid[1], Mostafa Toni[1,2] and Amir Ismail [1]

[1] *Geology Department, Faculty of Science, Helwan University, 11795, Ain Helwan, Cairo, Egypt.*

[2] *National Program for Earthquakes and Volcanoes, Geohazard Center, Saudi Geological Survey, Jeddah, Saudi Arabia.*

ARTICLE INFO

Keywords:

ERT,
SSR,
Geotechnics,
New-Cairo,
Egypt

ABSTRACT

The Egyptian government is active in multiple areas designated for industry and urban development on the outskirts of both the capital and various governorates within newly established cities. The proposed site for the creation of the industrial zone of New-Cairo City is regarded one of Egypt's most promising commercial and combined services zones. The study's primary goal is to map the region's subsurface geological conditions and interpret the findings for geotechnical qualities of the underlying materials. The study aims to evaluate the properties of the subsurface layers to determine their suitability for construction and engineering purposes. This research represents a case study that focuses specifically on the combined services area of Madinaty, to assess the suitability of the subsurface layers for geotechnical engineering purposes. To gather data about the subsurface layers, the investigation employed two geophysical techniques: Electrical Resistivity Tomography (ERT) and Shallow Seismic Refraction (SSR). SSR is used in the study area to identify dynamic geotechnical characteristics of the base layers using the P-wave and S-wave velocities. Two sub-surface layers are identified based on the velocity values of the Geo-seismic layers. The first layer is composed of mixed soil of sand, clay, and gravel, where the second layer composes of hard Limestone. According to all the criteria, regarding engineering aims, the area is divided into high, moderate, and low competent-material zones with varying degrees of fittingness. The current study suggested sorting the fundamental subsurface materials in the high and moderate zone for engineering purposes.

* Corresponding author at: *Geology Department, Faculty of Science, Helwan University, 11795, Ain Helwan, Cairo, Egypt.*
alhussein.adham@science.helwan.edu.eg

Journal of Applied Geophysics (Cairo): A Peer review journal, ISSN: 1687-1251
doi: 10.21608/JAG.2023.207522.1001

1. Introduction

Urban planners often neglect studying the soil properties of industrial cities, assuming that these areas do not require such studies due to the lower load and height of combined service area buildings compared to residential buildings. However, the industrial city in New-Cairo has become increasingly popular among investors, and the current study aims to address the absence of geotechnical information in the area due to its economic significance and growing workforce. The combined services area of Madinaty city is located between Latitudes 30° 6' 15.0372" N and 30° 6' 26.2296" N and Longitudes 31° 36' 40.5216" E and 31° 37' 52.6728" E and it covers a perimeter of about 1.16 km and an area of about 0.62 Km^2 (Fig. 1).The Electrical Resistivity Tomography (ERT) method measures the electrical resistivity of the subsurface layers. The ERT model and its subsurface layers are very similar to the model derived from the Shallow Seismic Refraction (SSR) method. The dynamic elastic moduli, which determines the soil's ability to withstand loads, can be possibly estimated by determining the velocity of the underground layers (Abd El-Rahman, 1991; Toni; 2007&2012; Basheer et al., 2012; El-Eraki et al., 2012; Biswas and Mondal, 2021; Li et al., 2021). However, cyclic dynamic loading can cause additional stress on the construction load, leading to concrete material overloading beyond the greatest high value of bearing capacity of the rock material. Soil competence measurements are lacking to evaluate the center of the machine's location in the entire area, including non-shaky/inactive and earthquake zones. Therefore, a geophysical method, such as shallow seismic refraction, can be used to quickly and cost-effectively survey the study area to assess its geotechnical parameters (Tezcan et al., 2007; Toni; 2007&2012; Adeep, 2010; keçeli, 2012; Wang and Wang, 2021; Wu et al., 2021).

In the current study, a shallow seismic refraction survey is done by taking 45 profiles to record Compressional (P-wave) and Shear (S-wave) velocities. Geological sequence information from five drilled wells inside the investigated area (drilling depth about 30m) is used to compare and connect with the measured wave velocities obtained from the survey. The survey results are then used to estimate the geotechnical characteristics of the study area through mathematical methods and classify it accordingly. Finally, the homogeneity of the detected subsurface layers from the two geophysical methods used in the study addresses the successful integration of the electric and seismic for such goals.

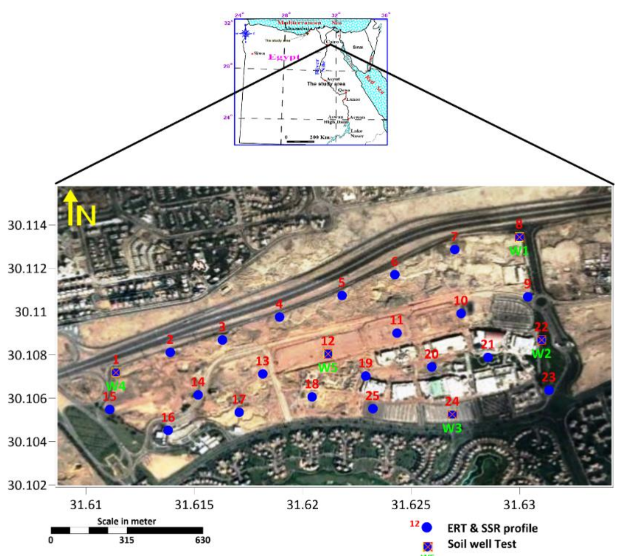

Figure 1. Location Map of the area under investigation showing sites of measurements.

2. Geological Setting and Stratigraphy

In the study area, the stratigraphic succession ranges from Oligocene to Miocene in geological age, as previously studied by Shukri and Akmal (1953). There are two stratigraphic sections: Upper Oligocene and Miocene (Fig. 2). The Upper Oligocene rocks include the Gebel El-Ahmer Formation, while the Miocene rocks consist of the Hagul Formation, which Shukri and Akmal (1953) named Marine and Non-Marine Miocene. Pliocene rocks lie unconformably over Miocene sediments. The Oligocene rocks are continental sands with silicified wood and gravels, and the central portion of the Cairo-Suez region is made up of high mountain ridges that extend in E-W and NW-SE directions, with lowlands in between. The stratigraphy of rock units is divided into pre-rift and syn-rift series based on their relationship to the Suez Gulf's rifting (Hammed and Khalek, 2015).
The examination of Oligocene rocks results in their classification into two units. The first unit is comprised of sand and gravel at the base, with a dark brown color and silicified wood trunks, while the second unit is made up of rift-related basaltic sheets at the top. The Oligocene elliptical dark hills and elongated ridges, which are a part of the syn-rift, are obscured by lag gravels and numerous basaltic rocks in the form of dikes cutting through the Eocene rocks and flows that are overlain by the Miocene strata. The Miocene rocks are divided into a basal unit consisting of marine Miocene materials such as marls, sandstones, shales, gravels, chalky limestones, and clays. Faults are the geological structures that impact the rocks in the study area, and there are three main fault sets: NW, EW, and NNW (Sadek, 1926; Said, 1990).

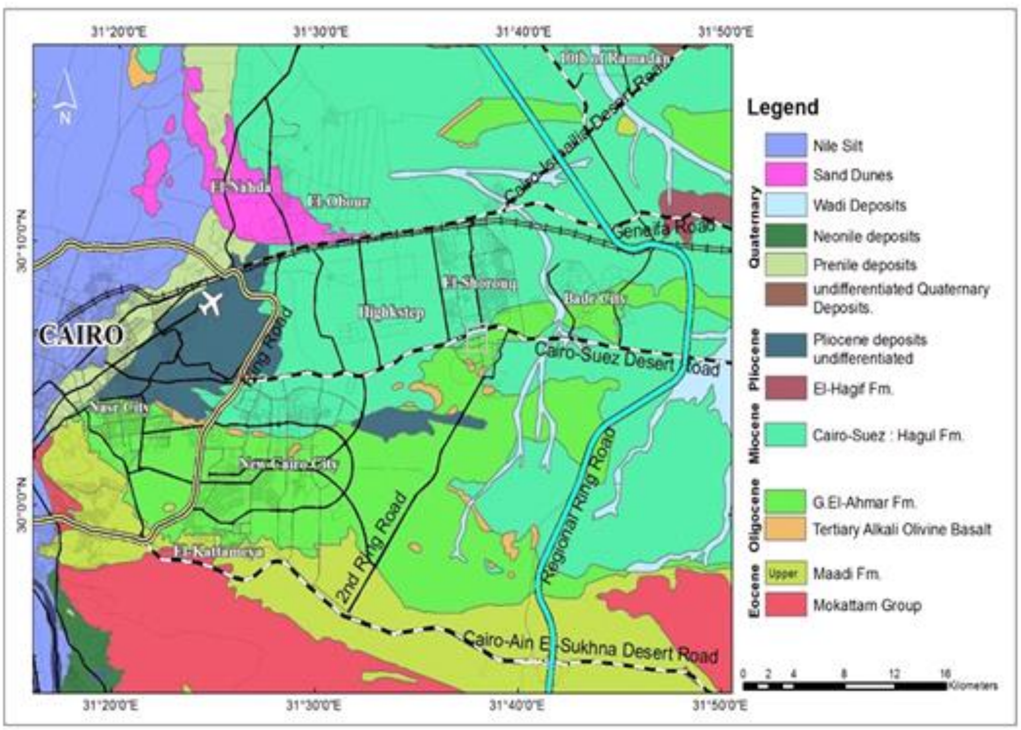

Figure 2. Geologic map of the studied area, (After Conoco, 1987).

3. Materials and Methods

3.1. Electrical Resistivity Tomography

Electrical Resistivity Tomography (ERT) is a geophysical tool that measures the electrical resistivity of subsurface materials. It involves injecting an electrical current into the ground and measuring the voltage response to create an illustration of the subsurface. The concept that ERT depends on is the variation of electrical conductivity and resistivity of different subsurface materials (Loke and Barker, 1996).

Different materials have different electrical conductivity and resistivity properties, and this affects the way they conduct electrical currents. By inserting an electrical current into the ground by two or more electrodes and measuring the resulting voltage, ERT can determine the resistivity of the subsurface materials (Nabighian and Macnae, 2005).

The ERT works by imaging the distribution of subsurface resistivity values by collecting electrical measurements along a series of closely spaced electrodes on the surface of the Earth. The measurements are then processed to create a 2D or 3D image of the subsurface resistivity distribution. This allows geologists, hydrologists, and other scientists to study the structure and composition of the subsurface, which can be useful in a variety of applications such as groundwater exploration, mineral exploration, and environmental studies (Sharma, 1997).

The ERT has several applications in site characterization, groundwater mapping, environmental monitoring, and geotechnical engineering. It can be utilized to find out the depth and thickness of subsurface layers and identify soil types and geological features. Also, the ERT can be utilized to assess the stability of slopes, identify potential landslide hazards, and design groundwater control systems for excavations and underground structures. Furthermore, ERT can be used to assess the condition of existing infrastructure, such as tunnels, pipelines, and retaining walls (Gupta and Roy, 2006; Gupta, 2021).

3.2. Shallow Seismic Refraction

The seismic technique is an approach that has been extensively used, especially in civil engineering, to determine the depth from the surface to the bedrock in various construction projects such as building huge structures, dams, highways, and harbors surveys (Valderrama, et al., 1996). Seismic refraction is the largely and commonly used reconnaissance technique for mapping shallow layer thicknesses and obtaining some lithology data. This method is useful for evaluating construction requirements and resolving issues related to sub-layers' geological nature (Telford et al., 1990). In order to perform seismic exploration, artificial seismic waves must be generated and recorded by geophones (Sharma, 1974). The activity of the Earth's surface, caused by energy source-points, is saved on a seismic record during seismic prospecting, using instrumental systems such as a geophone, amplifier, digital recorder, and monitoring units (Badley, 1985; Slotboom et al., 1996).

The survey approach used a variety of geophone spread systems, and in the present study area (i.e., combined services area of Madinaty city), a survey was conducted with 45 seismic refraction profiles totaling 135 seismic shots. Each profile used 48 geophones with 13 Hz as long as 240 m with 5 m in-line spread type geophones and shot points. The shot points' relative placements are varied in three alternative configurations: Normal, Middle, and Reverse arrangements. In normal and reverse shootings, the shot point is located 5 meters away from the first and last geophone respectively. All seismic profiles are oriented from North to South.

The following is a description of the devices used during seismic refraction surveys:

1. To generate P and S waves, a vibration generator device (3B Scientific U56001 Vibration Generator, 0 to 20kHz Frequency) has been used to transfer energy through the surface and layers of Earth.
2. Sensitive geophones are used to pick up the particles' motion created by the arrival of the seismic wave at surface of the ground (Thompson and Gist, 1993; Stokoe and Santamarina, 2000; Bashir et al., 2023). These geophones transform mechanical movement of ground particles to electrical signal with voltage amplitude relational to the obtained energy.
3. Vertical geophones (13 Hz) have been utilized to record P waves, while horizontal geophones are utilized to record S waves (4.5 Hz). The geophones are placed in two rows and fixed in the soil for the measurement area.
4. Electric signals are moved during cables to the record data system from the ground motion generated by the vibration generator and picked up by the geophones. The recording system consists of filtering and amplification options of the logged signal. The seismograph record system is called "GEOMETRICS, SMARTSEIS," a 48-channel seismograph powered by a 12 V DC battery and has a temperature range from 0 to 45 degrees Celsius.

5. To prevent dropping the wave force that could occasionally result from the blind layer, the force of the vibration generator is employed. The analog-to-digital conversion circuit is placed in front of a low-pass filter with a response of 7–10 MHz in the recording system. The vibration generator is first put into S-wave mode for a "45-degree pulse" at the picking point. The P-waves are delayed and become weaker due to them spreading out in the "air" with high weak wave conduction. S-waves will make up the majority of waves that geophones can detect. A software program (Winsism™ version 16 and Seisimager Version 3.3) can digitally separate S-waves and P-waves, in another arithmetic sense, S-waves have smaller values than P-waves.

3.3. Geotechnical Parameters

By analyzing the arrival times and amplitudes of seismic waves generated by a controlled source, geotechnical engineers can calculate important parameters related to the strength, stability, and deformation properties of the subsurface materials. These parameters are crucial for a range of engineering purposes, including site characterization, slope stability analysis for determining the appropriate angle of repose, geotechnical modeling for evaluating the stability of slopes and embankments, groundwater presence for determining the depth and thickness of the aquifer, as well as the properties of the overlying and underlying soil layers, and inputs for numerical models to design foundations that will be able to safely support the loads of the structures. This information can help simulate the behavior of the subsurface materials under different loading and environmental conditions. By understanding the properties of the subsurface materials, engineers can design structures that are safe, efficient, and cost-effective.

4. Data Processing and Results

The common data processing steps involved in the ERT method include data quality control, data filtering, data correction, data inversion, model validation, and interpretation. Before processing the ERT data, it is crucial to check its quality, such as missing data, instrument noise, and electrode contact issues. Filtering techniques can then be applied to remove any noise present in the data. Various corrections can be applied, such as drift correction, electrode coupling correction, and temperature correction.

The inversion of ERT data involves generating a 2D or 3D image of the subsurface based on the electrical resistivity distribution, which can be carried out using different inversion techniques such as RES2DINV software. It is essential to validate the ERT model by comparing the inversion results with known subsurface information, such as borehole data, geologic maps, or other geophysical measurements. Finally, the interpretation can involve identifying and characterizing subsurface features, such as faults, fractures, mineral deposits, or groundwater.

The shallow seismic refraction technique uses seismic waves to ascertain the ground underlying structure. Once the data of shallow seismic refraction has been collected, it must be processed in order to yield relevant subsurface information. The common data processing techniques for shallow seismic refraction data include: (1) Velocity analysis is utilized to regulate the average seismic velocity of subsurface layers, (2) Refraction statics correction is necessary to correct for the effects of near-surface velocity variations on the travel times of seismic waves, (3) The time-distance curve can be utilized to identify the depth and thickness of subsurface layers, (4) Tomography is a technique used to create a two-dimensional image of the subsurface based on seismic velocities, (5) Depth conversion is used to convert the travel times of seismic waves to depth values using the velocity model obtained from the data processing techniques. These data processing techniques are important for interpreting shallow seismic refraction data and obtaining accurate information about the subsurface structure.

4.1. ERT Cross-Section

The resistivity imaging's electrical cross-sections illustrate changes in resistivity values with measurement depth, which can be affected by various factors such as lithology, soil grain size, water content, moisture content, and rock porosity and permeability. The resistivity values of the upper layer are influenced by the variety of soil types present in it, which is determined by the proportion of each rock component.

The RES2DINV program was utilized to present the two-dimension (2D) ERT data, which created two cross-sectional images (Fig. 3a & b) that display an example for the iterated and interpreted real resistivity of ERT profile in two dimensions. The values of apparent resistivity and depth for the sections were found to be regular and consistent with the information collected from the tested well in the analyzed region.

The first layer consists of a mix of sand, clay, and gravel soils with resistivity values that fall in between the other two layers. The second layer comprises hard limestone with high resistivity values.

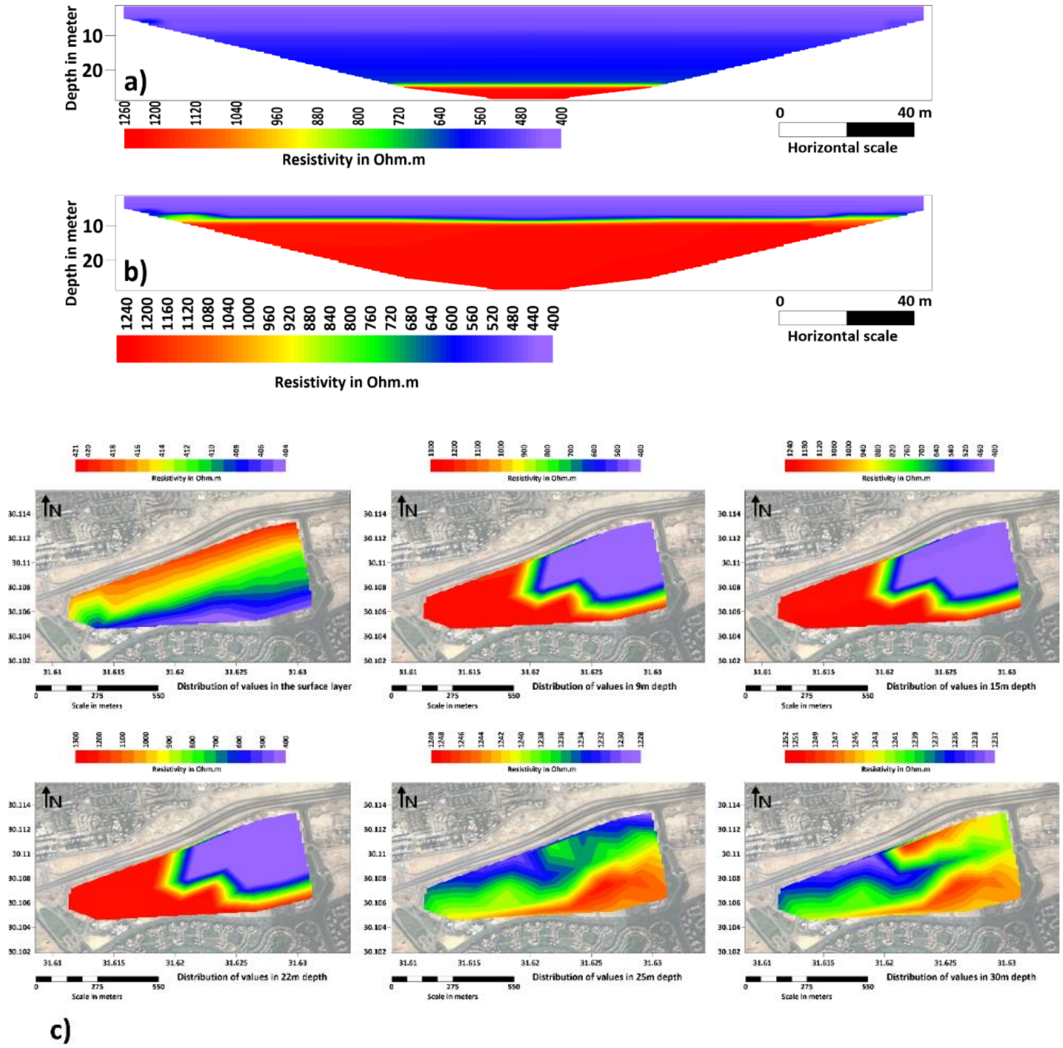

Figure 3. a) ERT Cross-section No. 1, b) ERT Cross-section No. 9, c) Three-dimension maps of ERT distribution at different depths over the area under investigation.

Upon examination of all 2D electrical imaging sections that encompassed the spot region, it was determined that two distinct layers could be identified based on similar electrical resistivity changes. Three-dimensional (3D) maps are constructed from 2D data using a technique called "3D inversion". This technique involves taking multiple 2D data sets and combining them to create a 3D image of the subsurface by using inversion algorithms. The Geoelectrical cross-sections and 3D maps (Fig. 3c) reveal a two-layer model with distinct resistivity values. These values were translated into two lithological layers based on Said's (1981) stratigraphic column. The first layer has a thickness of 9 meters and resistivity values that range from 403 to 423 Ohm.m. It consists of a mix of sand, clay, and gravel soils with resistivity values. Whereas the second layer has a thickness of about 8 meters and resistivity values ranging from 1228 to 1249 Ohm.m. It comprises hard limestone with high resistivity values. The second layer exhibits an increase in resistivity and may serve as a critical boundary for construction in the area. Notably, the sequence of resistivity readings indicates no unusual variations in the homogenous layers, suggesting the absence of clay lenses.

4.2. Geo-Seismic Data

Graphing of the time-distance relationship showed that there is a clear distinction for the presence of two layers in the study area (Fig. 4 a & b). The same two geo-seismic layers can be distinguished based on the vertical dispersion of the P and S waves with depth (Fig. 4 c & e) and the lithological sequence of a soil test well (Fig. 4 d). Figure (5a) shows the P-wave velocity distribution over the study area, while S-wave velocity distribution has been shown in Figure (5b). Table (1) shows the amount and extent of the change of seismic velocities with depth in each of the two geo-seismic layers. From the distribution of velocities, according to the soil type classification of the International Building Code (IBC, 2006) by International Code Consortium (ICC, 2006) and The National Earthquake Hazards Reduction Program (NEHRP, 2021). It is noted that the first layer can be classified as dense soil or crumbly rocks (site class C), while the second layer is classified as coherent rock (site class B).

Table 1. The distribution of Vp and Vs with depth over the area under investigation.

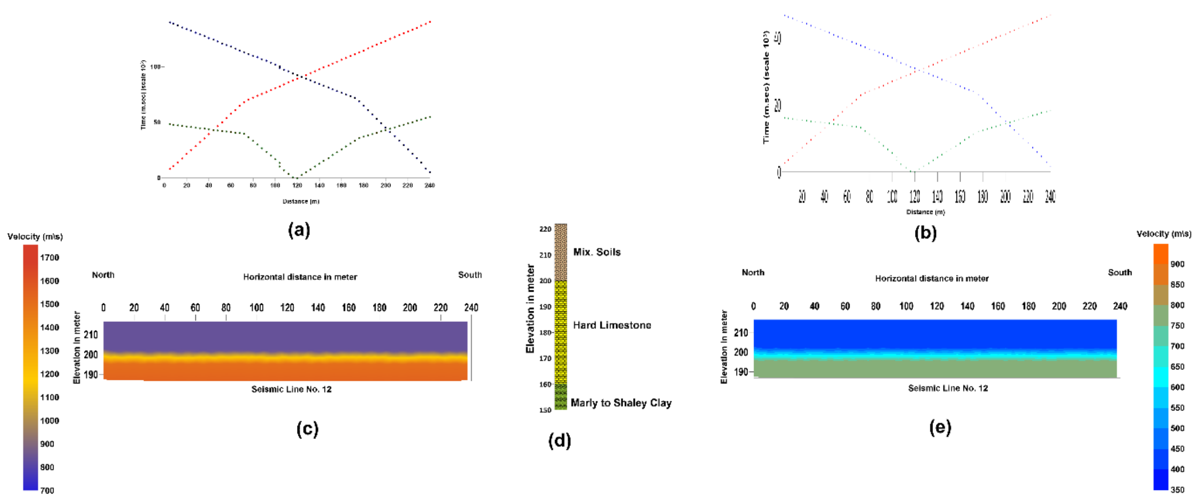

Geo-seismic layer	Depth	Vp range in m/sec	Vs range in m/sec
First layer	Surface to 21.5 m	810 to 863	427 to 453
Second layer	22m to 30 m	1510 to 1632	744 to 795

Figure 4. a) Time-Distance curve of Vp in seismic line No. 12, b) Time-Distance curve of Vs in seismic line No. 12, c) the vertical distribution of the Vp in seismic line No. 12, d) the lithological sequence of a soil test well No. 5, e) the vertical distribution of the Vs in seismic line No. 12.

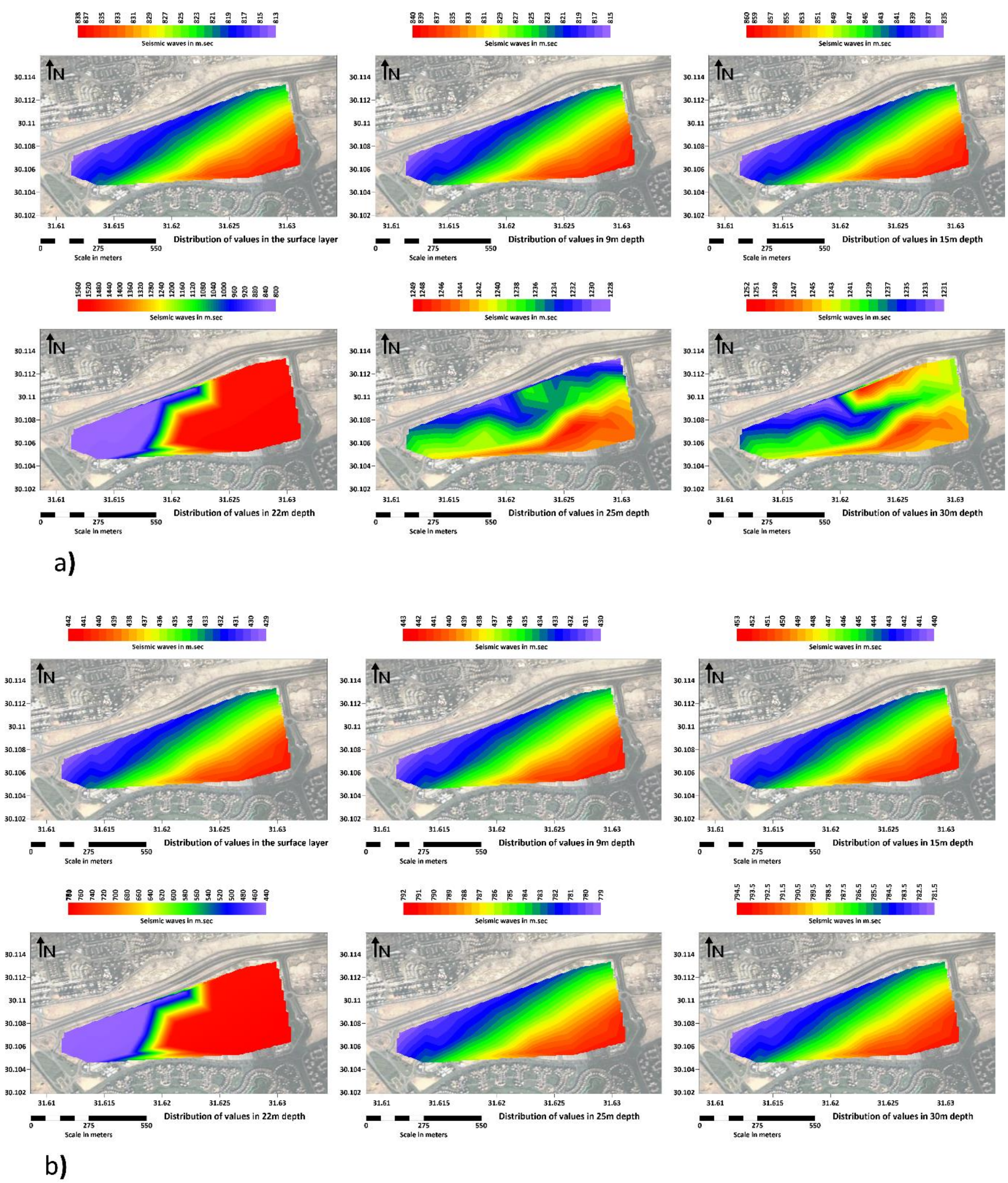

Figure 5. a) Three-dimension maps of P-wave velocity distribution at different depths over the area under investigation, b) Three-dimension maps of S-wave velocity distribution at different depths over the area under investigation.

4.3. Geotechnical Characterizations of the Foundation Material

The seismic approach is now widely used in civil engineering applications as a vital tool to estimate elastic deformation by calculating elastic modules. The technique involves measuring the speed of base rock during both natural and artificial cyclic dynamics to determine the specified elastic dynamic coefficient (Stumpel et al., 1984; Tezcan et al., 2007; Aoki and Matsukura, 2008; Adeep, 2010; keçeli, 2012; Andersen and Schjetne, 2013). This coefficient is then used to compute the additional load on the structure, which helps identify the maximum load that subsurface rock materials can bear (Bowles, 1984). Unfortunately, the soil competency scales created using the collected and analyzed samples are not fully representative of the research region, making it difficult to analyze calm areas and those affected by earthquakes. Soil, in the context of building engineering, is referred to as the substance that encompasses the rock layer below, which was created by the process of weathering. (Abd El-Rahman 1991; Abd El-Rahman et al., 1992; Azimian, et al., 2014; ASTM, 2015). The mechanical properties of soil are determined by the elastic characteristics of the material, which can be determined using conventional engineering techniques or field measurements by geophysical tools (Sjorgren et al., 1979; Dutta, 1984). This study used shallow seismic refraction readings of compressional and shear wave velocities (Vp and Vs) to analyze the foundation rock in the study area and determine geotechnical moduli, parameters, and characteristics as listed in Table 2.

Table 2: Classification includes all the estimated elastic moduli, material competence, and bearing capacity of the foundation materials.

Mechanical Properties		**First Layer**		**Second Layer**	
		from	**to**	**from**	**to**
Elastic moduli	**Poisson's ratio**	0.30685	0.3085	0.307	0.31986
	Kinetic rigidity modulus	348	438	0	4250
	Kinetic young's modulus	910	1150	0	11200
	Kinetic bulk modulus	785	1000	0	10400
	N-value	97	114.5	60	595
Material competence	**Material index**	-0.2312	-0.2302	-0.28	-0.2784
	Concentration index	4.249	4.2515	4.125	4.1289
	Stress ratio	0.4426	0.4461	0.443	0.47028
	Density gradient	$2.26x10^{-6}$	$2.3x10^{-6}$	$6x10^{-7}$	$6.74x10^{-7}$

Foundation material bearing capacity	**Ultimate bearing capacity (K.Pa)**	2910	3430	2000	17850

5. Conclusion and Recommendation

This study aims to describe the underground geological conditions and interpret geotechnical properties of foundation rock components in the combined services area of Madinaty, new Cairo. It involved analyzing electrical resistivity tomography (ERT) and shallow seismic refraction (SSR) data using 45 measuring sites for each tool.

The study also identified dominant structural patterns in the study area that should be avoided during city and highway design to prevent damage from earthquakes or overburden caused by vehicles. The study's findings reflect its objectives and are relevant to civil engineering and other applications.

This study helped focus on the fact that using both electrical resistivity tomography and shallow seismic refraction methods in engineering surveys can provide complementary information about the subsurface conditions. The ERT is a useful tool for mapping the distribution of different subsurface materials based on their electrical resistivity, which can help identify variations in lithology, moisture content, and other geotechnical properties. Shallow seismic refraction, on the other hand, can provide information about the elastic properties of the subsurface, such as the seismic velocity, which can be used to estimate the depth and thickness of different layers, geotechnical parameters and to infer their mechanical strength and load-bearing capacity.

By combining the results of these two geophysical methods and with helping drilled wells for rock tests, it is possible to obtain a more comprehensive picture of the subsurface conditions and to improve the accuracy of geotechnical models and design parameters for engineering purposes, such as site characterization, foundation design, and slope stability analysis. ERT can help identify zones of high moisture content or clayey soils that may be prone to liquefaction during seismic events, while SSR can help estimate the depth of bedrock or other competent layers that can provide adequate support for foundations or retaining structures. Overall, the integration of ERT and SSR methods can lead to better informed decisions and more effective engineering solutions.

This study emphasizes that the geophysical methods used in the investigation have provided consistent and agreeable indications regarding the soil composition, the number of sequences, and the geotechnical properties of the subsurface layers. This indicates that the results obtained from these geophysical methods are reliable and can be used for geotechnical and engineering purposes, such as determining the foundation design and construction methods for a particular site. Generally, the use of multiple geophysical methods can increase the accuracy and reliability of subsurface investigations by providing complementary information and validating the results obtained from each method.

The study identified two lithologic layers, based on ERT and SSR data interpretations: The first layer composed of mixed soils while the second layer composed of limestone. The seismic refraction method is used to classify the foundation rock material in the study area. It was concluded that it is necessary to exclude the first surface layer for any of the purposes of building or facilities, and to nominate the building on the second layer. From the studies of the technical properties, the second layer was divided into three zones according to each of its thickness and geotechnical parameters (Table 1 and Fig. 6) as:

1. Zone A: Suitable for any engineering purposes.
2. Zone B: Suitable for limited buildings.
3. Zone C: Unsuitable for construction.

The study also identified dominant structural patterns in the study area that should be avoided during city and highway design to prevent damage from earthquakes or overburden caused by vehicles. The study's findings reflect its objectives and are relevant to civil engineering and other applications.

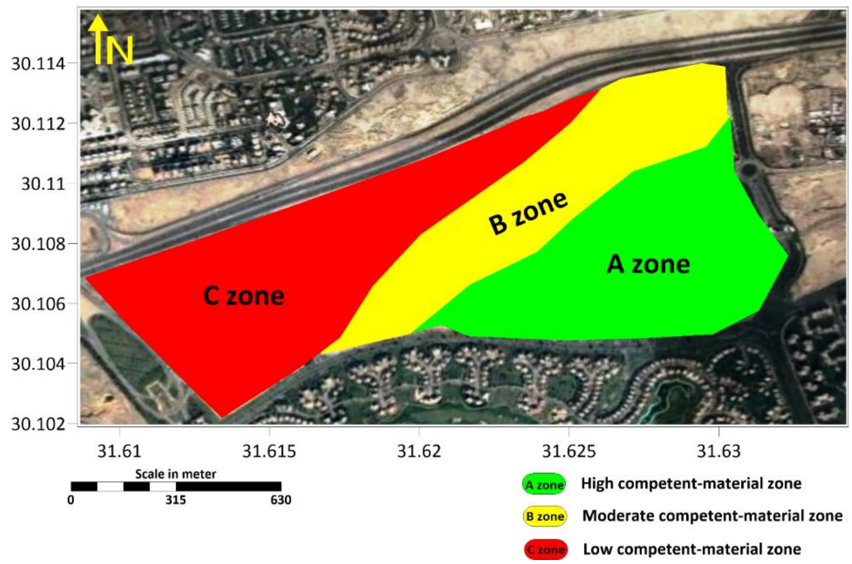

Figure 6. Classifications of zones in the second layer of the investigated area according to the distribution of geotechnical characteristics and properties of electrical resistivity.

Declaration of interest

The corresponding author discloses any potential competing or non-financial interests on behalf of all authors of the work.

6. References

Abd El-Rahman, M. (1991). Rock material competence assessed by seismic measurements with emphasis on soil competence scale and applications in some urban areas in Yemen. EGS. Proc. of the 9th Ann. Meet., pp. 206-228.

Abd El-Rahman, M. M., Setto, I., El-Werr, A. (1992). Inferring mechanical properties of the foundation materials at the2nd industrial zone, Sadat City, from Geophysical measurement, EGS. Proc. of the 10th. Ann. Meet. 10, PP.50-62.

Adeep, S. (2010). Housing Economics under Market Mechanisms, Cairo University – Faculty of Engineering, 2010.

Andersen, K.H., and Schjetne, K. (2013). Database of Friction Angles of Sand and Consolidation Characteristics of Sand, Silt, and Clay," Journal of Geotechnical and Geo-environmental Engineering, ASCE, Vol. 139, No. 7, pp. 1140-1155. DOI: 10.1061/(ASCE)GT.1943-5606.0000839.

Aoki, H., and Matsukura, Y. (2008). Estimating the unconfined compressive strength of intact rocks from Equotip hardness," Bulletin of Engineering Geology and the Environment, Springer-Verlag, Vol. 67, No. 1, pp. 23-29. DOI: 10.1007/s10064-007-0116-z.

ASTM D2573. (2015). Standard Test Method for Field Vane Shear Test in Saturated Fine-Grained Soils, ASTM International. DOI: 10.1520/D2573_D2573M-15.

Azimian, A., Ajalloeian, R., Fatehi, L. (2014). An Empirical Correlation of Uniaxial Compressive Strength with P-Wave Velocity and Point Load Strength Index on Marly Rocks Using Statistical Method, Geotechnical and Geological Engineering, Vol. 32, No. 1, pp. 205-214. DOI: 10.1007/s10706-013-9703-x.

Badley, M.E. (1985). Practical seismic interpretation: Boston, International Human Resources Development Corp.,266 p.

Basheer, A.A., Atya, M.A., Shokri, M., & Abu shady M.M. (2012). Application of ERT and SSR to detect the subsurface cave at 15th May City, Helwan, Egypt, NRIAG Journal of Astronomy and Geophysics (2012), 1, Available online 20 January 2013, pp. 23–32.

Bashir, S., Chowdhary, A. R., Akhtar, N. (2023). Prediction and attenuation of ground vibrations generated by moving trains. Current Science (00113891), 124(2).

Biswas, A., and Mondal, A. (2021). Assessment of the stability of slopes using electrical resistivity tomography and slope stability analysis. Geomechanics and Engineering, 25(1), 1-13.

Bowles, J.E. (1984). Physical and Geotechnical properties of soil. McGraw-Hill London, P. 477-480.

Conoco, C. (1987). Geological map of Egypt, scale 1: 500,000-NF 36 NE-Bernice, Egypt. The Egyptian General Petroleum Corporation, Cairo.

Dutta, N.P. (1984). Seismic refraction method to study the foundation rock of a dam. Geophysical Prospecting, 32.1103-1110.

El-Eraki, M., Mohamed, A. A., El-Kenawy, A. A., Toni, M. S., Shimaa, I. M. (2012). Engineering seismological studies in and around Zagazig city, Sharkia, Egypt. NRIAG Journal of Astronomy and Geophysics, 1(2), 141-151. DOI:10.1016/j.nrjag.2012.12.009

GEOMETRIC SMARTSEIS system [Computer Software], (2015). Geostuff, 1579 Lupine Lane Lincoln,California 95648 USA, user manuals and applications, ftp://geom.geometrics.com

Gupta, H. K. (2021). Artificial water reservoir-triggered earthquakes, with special emphasis on Koyna, India. In Encyclopedia of Solid Earth Geophysics (pp. 19-32). Cham: Springer International Publishing.

Gupta, H. K., and Roy, S. (2006). Geothermal energy: an alternative resource for the 21st century. Elsevier.

Hammed, M. S. and Khalek, A. A. (2015). 3D digital geological mapping and lithological characterization of the northwestern margin of the gulf of suez, egypt by integration of remotely sensing data. Proceedings of the 15th International Multidisciplinary Scientific GeoConference SGEM 2015, 1, 11-22.

IBC (2006). International Building code, http://bcpad.net/Code%20Books/IBC%202006.pdf

ICC (2006). International Code Consortium, https://www.iccsafe.org/

Keçeli, A. (2012). Soil parameters which can be determined with seismic velocities. Jeofizik, 16(1), 17-29.

Li, Q., Lin, J., Wang, H., Yan, B. (2021). Investigation of the subsurface structure and groundwater flow using electrical resistivity tomography and pumping tests: A case study in China. Journal of Hydrology, 597, 126131.

Loke, M.H., and Barker, R.D. (1996). Rapid least-squares inversion of apparent resistivity pseudosections by a quasi-Newton method1. *Geophysical prospecting*, *44*(1), 131-152.

Nabighian, M.N., and Macnae, J.C. (2005). Electrical and EM methods, 1980–2005. *The Leading Edge*, *24*(Supplement), S42-S45.

NEHRP. (2021). National Earthquake Hazards Reduction Program, https://crsreports.congress.gov/product/pdf/R/R43141.

RES2DINV [computer software] (2021). Landviser company, inlghting research, https://landviser.com/software/res2dinv/

Sadek, H. (1926). The geography and geology of the district between Gebel ʻAtâqa and El-Galâla El-Baharîya (Gulf of Suez).

Said, R. (1990). The geology of Egypt: balkema. Rotterdam, Brookfield, 734.

Seisimager Version 3.3. [Computer Software] (2015). Jean-Luc Arsenault, USA, software

SeisImager/2D. ftp://geom.geometrics.com/pub/seismic/SeisImager/.

Sharma, P.V. (1974). Geophysical Methods in Geology. New York, Elsevier, 428 P.

Sharma, P.V. (1997). Environmental and engineering geophysics. Cambridge university press.

Shukri, N. M. and Akmal, M. G. (1953). The geology of Gebel el-Nasuri and Gebel el-Anqabiya district. Bull. Soc. Geogr. Egypte, 26, 243-276.

Sjogren, B., Ofsthus, A., Sandberg, J. (1979). Seismic classification of rock mass qualities. Geophysical Prospecting, 1979, 27: P. 409-422.

Slotboom, R.T., Lawton, D.C., Spratt, D.A. (1996). Seismic interpretation of the triangle zone at Jumping Pond,Alberta: Bulletin of Canadian Petroleum Geology, vol. 44, p. 233–243.

Stokoe, K. H., and Santamarina, J. C. (2000). Seismic-wave-based testing in geotechnical engineering. In ISRM international symposium. OnePetro.

Stumpel, H., Kahler, S., Meissner, R., Milkerei, B. (1984). The use of seismic shear waves and compressional waves for lithological problems of shallow sediments: Geoph. Pros.,1984, 32, P.660-675.

Telford, W.M., Geldart, L.P., Sheriff, R.E. (1990). Applied Geophysics: Cambridge, Cambridge University Press, 770p.

Tezcan, S. S., Ozdemir, Z., Keceli, A., Erkal, A. (2007). A rapid technique to determine allowable bearing pressure. In International Earthquake symposium Kocaeli.

Thompson, A. H., and Gist, G. A. (1993). Geophysical applications of electrokinetic conversion. The leading edge, 12(12), 1169-1173.

Toni, M. (2007). Geotechnical and site effect studies in Hurghada city, Red Sea, Egypt. M.Sc. thesis, Faculty of Science, Assiut University, Egypt.

Toni, M. (2012). Site response and seismic hazard assessment for the southern part of Cairo city, Egypt. PhD dissertation, Faculty of Science, Assiut University, Egypt.

Valderrama, M.H., Nielsen, K.C., McMechan, G.A. (1996). Three-dimensional seismic interpretation from the triangle zone of the frontal Ouachita Mountains and Arkoma basin, Pittsburg County, Oklahoma: AAPG Bulletin,vol. 80, p. 1185–1202

Wang, Q., Xie, W., and Wang, X. (2021). Investigation of subsurface geological structures using the shallow seismic refraction method: A case study in China. Journal of Applied Geophysics, 187, 104318.

Winsism™ version 16 [Computer software] (2018). Winshttp://www.wgeosoft.ch /PDF/winsism_pub_us.html

Wu, X., Wu, J., Liu, Y., Xu, C., Zhang, Q. (2021). Evaluation of concrete strength using electrical resistivity tomography. Construction and Building Materials, 303, 124603.